11-29-2011

Design of a Metatarsophalangeal Joint Implant Wear Tester

Kelly Wilton Schlachter

DESIGN OF A METATARSOPHALANGEAL JOINT IMPLANT WEAR TESTER

by

Kelly W. Schlachter

A Thesis

Submitted in Partial Fulfillment of the

Requirements for the Degree of

Master of Science

Major: Mechanical Engineering

The University of Memphis

December 2011

Abstract

Schlachter, Kelly Wilton. MSME. The University of Memphis. December 2011. Design of a Metatarsophalangeal Joint Implant Wear Tester. Major Professor: Dr. Gladius Lewis.

The purpose of the present study was to design a wear tester for implants of the first metatarsophalangeal joint (FMTPJ), otherwise known as the first joint of the big toe. Many different designs of this type of implant from many manufacturers are currently in clinical use, but there is no information in the open literature as to how these implants are tested for *in vivo* durability. There are several case studies, however, in which premature implant fractures were reported. It is possible that the incidence of such fractures might have been lower if standardized wear testing of FMTPJ implants existed. We studied the development history of FMTPJ implants, the designs of implants currently in clinical use; current wear test methods used on hip and knee implants, the biomechanics of the FMTPJ, and designed a wear tester that could be used to test current and future implant designs *in vitro*. A stress analysis of the tester indicated that any failure would occur at the implant/fixture interface and that the machine can test at forces beyond what has been observed in the normal gait.

TABLE OF CONTENTS

List of Figures iv

Introduction 1

Background and Motivation 1

Study Purposes 2

Background 3

Anatomy of the FMTPJ 3

Physiology of the FMTPJ 4

Kinematics and Kinetics 5

Pathophysiology of the FMTPJ and Treatment Options 7

FMTPJ Implant Designs 9

Design, Operation, and Stress Analysis 11

Design Requirements for the Wear Tester 11

Details of the Designed Wear Tester 11

Operation of the Designed Wear Tester 17

Stress Analysis of an Articulating Test Station 18

Proposed Wear Test Protocol 22

Conclusion 25

References 27

List of Figures

Figure 1. Medial View of the Right Foot 3

Figure 2. Schematic Diagram Showing Key Features of the FMTP joint 4

Figure 3. Motions of the Foot 5

Figure 4. The Normal Gait Cycle 6

Figure 5. 2D Schematic Drawing of Wear Tester 13

Figure 6. Solid Model of the Assembled Wear Tester 14

Figure 7. Solid Model of Cut-Away View of One of the Articulating Stations 15

Figure 8. Solid Model: Close-Up View of Implant Mounted in the Wear Tester 16

Figure 9. Solid Models of the Component Mounts 17

Figure 10. 0^o Meshed Structure 19

Figure 11. 40^o Meshed Structure 19

Figure 12. 0^o 1200N Load 20

Figure 13. 40^o 1200N Load 20

Figure 14. von Mises Stress Contour for a Test Station, at 0^o Articulation 21

Figure 15. von Mises Stress Contour for a Test Station at 40^o Articulation 22

Introduction

Background and Motivation

There is no doubt that the great toe is the most important digit in the foot. When it comes to balance and propulsion, the great toe shoulders the majority of the loads placed on the digits, with the lesser toes balancing out the rest (1). The first joint of the big toe, called the first metatarsophalangeal joint (FMTPJ), is affected by many degenerative diseases. At the later stages of these diseases, a treatment that is widely used to alleviate pain and to restore joint function is a FMTPJ implant.

Total joint replacements have been around since the late 1800s (2). The earliest recorded total hip joint replacements (THJRs) and total knee joint replacements (TKJRs) were performed around 1891 (2). Today, there are approximately 200,000 THJRs and 500,000 TKJRs implanted in the United States every year (jisrf.com). These arthroplasties are well established surgical procedures and the implants associated with these procedures have been extensively tested using international standards; namely, ISO14242 (3) and ISO14243 (4). These standards contain, among other things, details of protocols for wear testing of an implant as well as of the method for determining the amount of wear.

In contrast to THJRs and TKJRs, there are currently no industry standards for the wear performance of FMTPJ implants. This is a consequence of the fact that, while there are many types and designs of FMTPJ implants and a large collection of manufacturers that design and/or fabricate/produce them, there is nothing in the open literature on wear testing of these implants. Just as a hip or knee implant, a FMTPJ implant articulates with

the contiguous bones or secondary components throughout its life and, thus, has potential for generating wear debris or for fracturing.

Hinged FMTPJ implants fabricated from a polysiloxane (Silastic®) have been around since the 1970s and are still popular in clinical use today (5). Failures of these implants have included deformation, fracture, and abrading (6,7). There are no long-term follow-up clinical data on metal hemi-implants and multi-component totals implants. There are, however, several case studies involving examination of explanted implants, in which excessive surface wear, debris in the surrounding tissue, and fracture, have been observed (8,9,10**).** Although the results of *in vitro* wear testing do not necessarily predict the life expectancy or the *in vivo* wear performance of an implant, they provide valuable insight into the wear resilience of the implant and may be used to screen sets of implant designs.

Study Purposes

The purposes of the present work were two-fold. The first was to design a FMTPJ implant wear tester whose motion cycles replicate those that occur at the joint during activities of daily living, especially walking, and is not only capable to use to evaluate implant designs that are in current clinical use but is also adaptable to test future implant designs. The second was to present the essential features of a protocol to be used with the designed tester.

Background

Anatomy of the FMTPJ

The foot is divided up into three sections; namely, the hind-foot, the mid-foot, and the fore-foot. There are 28 bones, 19 intrinsic muscles, 38 tendons, and over 100 ligaments in the foot and ankle (11). The hind-foot includes the heal, the mid-foot includes the arch of the foot, and the fore-foot includes the metatarsals and phalanges of the toes (Figure 1). The FMTPJ comprises the metatarsal and proximal phalanx bones and, to a lesser degree, the sesamoids (Figure 2). Several ligaments surround the joint for stabilization, including the medial collateral, lateral collateral, and plantar ligaments (6). The extensor hallucis longus and brevis are the tendons responsible for dorsiflexion, the flexor hallucis longus and brevis are responsible for plantarflexion, the abductor hallucis are responsible for abduction, and the adductor hallucis are responsible for adduction (11,12). The FMTPJ is composed of a cartilage-lined metatarsal head and phalanx base to allow "frictionless motion" and is also surrounded by a capsule for static stability (13).

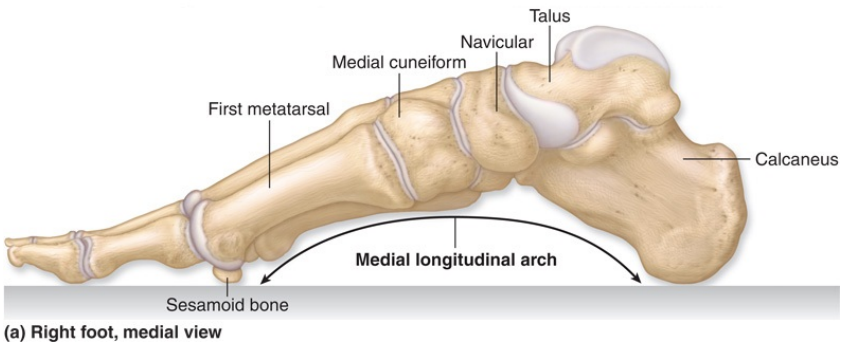

Figure 1. Medial View of the Right Foot (14).

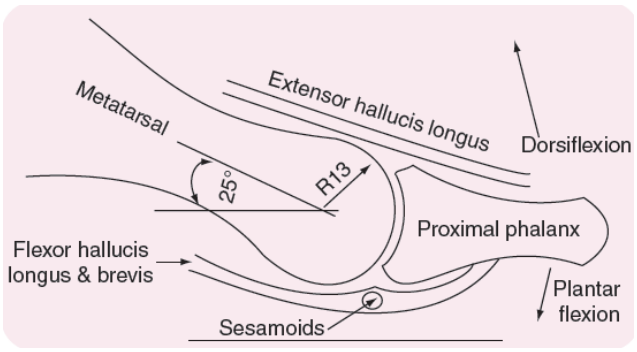

Figure 2. Schematic Diagram Showing Key Features of the FMTP joint (6).

Physiology of the FMTPJ

Feet are the structural supports of the body that allow upright locomotion and are designed to handle repetitive loads of multiples of bodyweight (11). The network of bones, ligaments, tendons, and muscles are able to adjust to different ground contours and provide acceleration. The fore-foot can experience loads up to 1.2 x bodyweight during toe push off in normal walking, with the FMTPJ taking up to bodyweight at its peak (15). The FMTPJ is capable of handling these loads while maintaining its normal functions of plantarflexion (lowering), dorsiflexion (raising), adduction (bringing toes together) and abduction (spreading toes apart) (16) as shown in Figure 3. The FMTPJ is also capable of being very flexible to allow bending and crouching, but can become rigid to transfer weight-bearing forces during propulsion (11). Motion includes the base of the phalanx gliding over the head of the metatarsal with the sesamoid bones, embedded in the flexor tendons, sliding over the joint and keeping the tendons from flattening out (11).

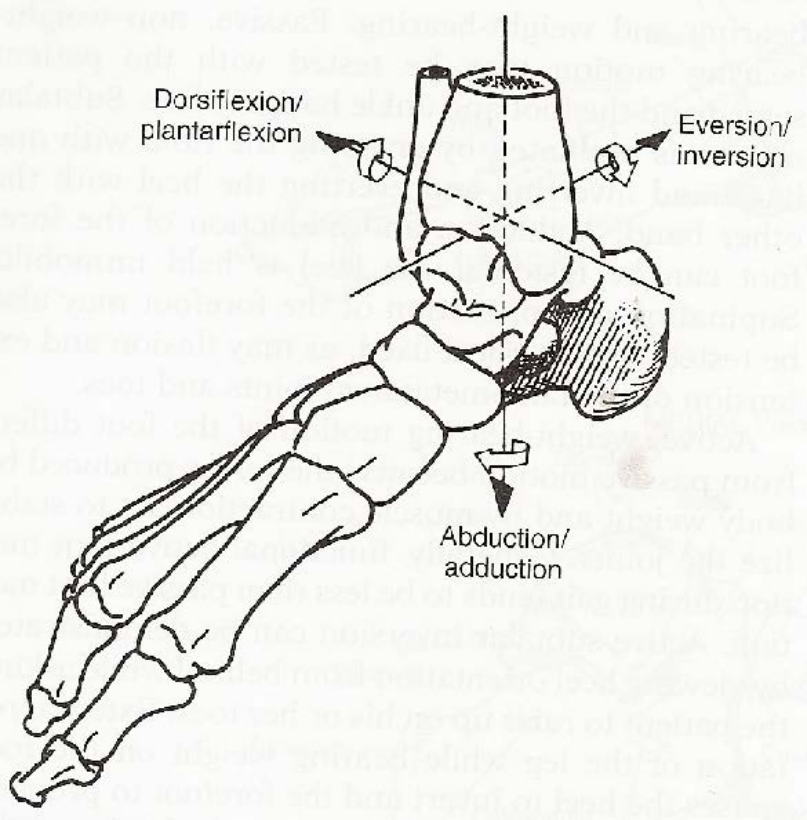

Figure 3. Motions of the Foot (11).

Kinematics and Kinetics

FMTPJ motion includes flexion, extension, adduction, and abduction (Figure 3) (11,17). Range of motion is discussed frequently in the literature as it is one of the primary parameters used to determine the stage of joint deterioration, which treatment option to use, and the success or otherwise of the treatment outcome (18-20). Normal passive range of motion for a FMTPJ ranges from 90^{o} dorsiflexion to 30^{o} planterflexion with respect to the metatarsal axis, which is already at about a 25^{o} angle with respect to the floor (11). The range of motion measured during walking is much less, but there are differences in opinion about the magnitude of the range. This is a consequence of the many different measurement/determination methods used (18,21,22).

Most of the literature reports on the determination of forces experienced by the feet during various activities of daily living have focused on the normal gait cycle (Figure 4). This cycle can be broken up into two phases, the stance phase and the swing phase (11). The stance phase is 62% of the cycle and starts with the heel striking the ground, then moves on to the foot going flat, heel rise and finally push off, or toe off (11). The swing phase is 38% of the cycle and includes acceleration, toe clearance, and deceleration (11). It is to be noted that the FMTPJ was the subject in only a few of the aforementioned studies.

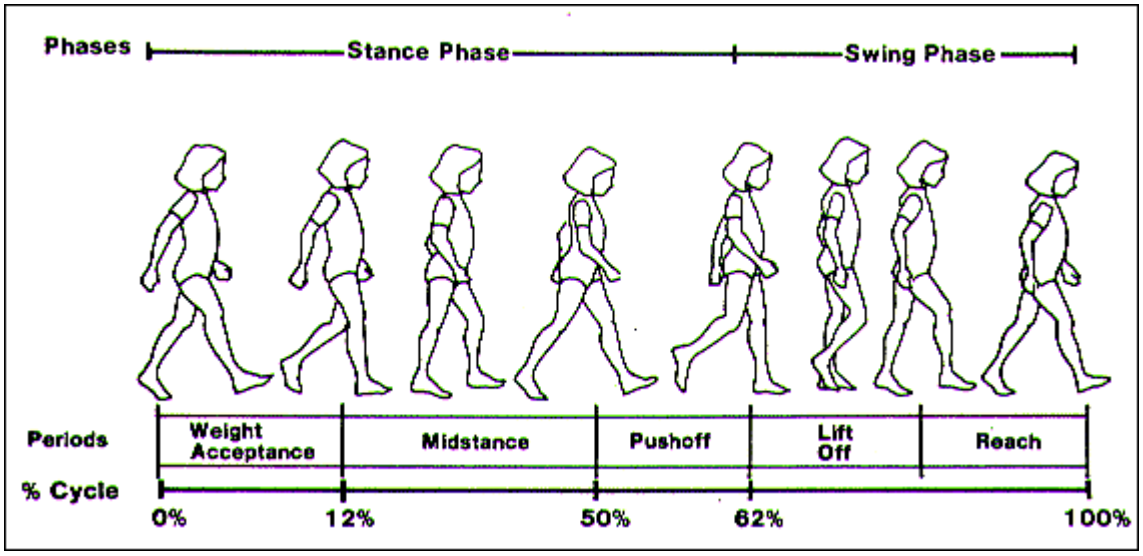

Figure 4. The Normal Gait Cycle (38).

Using radiographs of healthy feet to determine the geometries of the fore-foot and the angles it made with the ground, during the gait cycle, Stokes et al (15), using vertical ground reaction forces, calculated the force across the FMTPJ to be comparable to body weight. Jacob (1) also calculated the force placed on the FMTPJ by measuring the vertical ground reactions during normal gait cycle, but refined the analysis by creating

free body diagrams of the known geometries of the bones and the tendons, and calculated the resultant force that acted on the first metatarsal head based on the reaction forces of these tendons. Jacob calculated the force to be around 86% of body weight (1).

Pathophysiology of the FMTPJ and Treatment Options

There are many ailments that affect the FMTPJ, examples being osteoarthritis, rheumatoid arthritis, trauma/fracture, gout, bone/tissue deformities, bone spurs, and failed previous joint operations (23-25). These ailments can lead to many disorders, such as hallux valgus (bunion), hallux rigidus/limitus (diminished range of motion), hallux varus (typically, a postoperative deformity), sesamoid disorders, pain, and cosmetic disorders (26). If left untreated, these problems may lead to physiologic compromises, such as severe pain, difficulty in walking and a limited choice when it comes to footwear.

The many treatment options that are available may be grouped into two categories; one involving joint preservation and the other joint destruction. Joint preservation procedures can further be classified as surgical and nonsurgical. The first options for patients with early symptoms usually involve a conservative approach, such as use of anti-inflammatory drugs, orthotics, splinting, and casting (27). The goals of these options are to provide pain relief and, possibly, to delay the need for surgery. When a disorder progresses beyond what can be treated non-surgically, joint preservation surgical procedures are recommended. These surgical procedures involve cheilectomy, or the removal of bone spurs; soft tissue correction to force the toe back into alignment; and osteotomy, which is the removal a section or wedge of bone to realign the FMPTJ joint (20,24,26,27). For late stages of degenerative diseases of the FMTPJ, the only options are, usually, joint destructive ones (19). Three of the most widely used of these options

are arthrodesis, which is the fusion of the FMTP; implant arthroplasty, the partial or full replacement of the FMTPJ with an implant; and joint resection arthroplasty (Keller procedure) (19,23).

The first reported arthrodesis was performed in 1852 (19,23). Since then, arthrodesis has become the preferred treatment for patients in the advanced stages of degenerative joint disease (28). The primary goal of this procedure is pain relief and to restore some function of the toe. With a successful arthrodesis, the patient is again able to place his/her full body weight on the foot because the fused joint is able to distribute the loads across both the metatarsal and the first phalanx (26). Although, as a result of the fusion, all joint motion is lost, the success rate of arthrodesis, as measured by, for example, long-term pain relief, is very high (19,23).

The goals of a FMTPJ implant is to relieve pain and to restore function at the joint (37). Because it preserves some range of motion, implant arthroplasty is considered a viable option for treating late- or end-stage degenerative diseases, especially in more active patients (16,29). Insurance companies are also starting to recognize that a FMTPJ implant is a viable alternative to arthrodesis and are beginning to cover the cost of the procedure (30,31). As improvements in designs are introduced and more favorable results are reported, more surgeons will consider implant arthroplasty for late stage joint degenerative disease in the FMTPJ (29).

Joint resection arthroplasty was introduced in the early 1900s and involves only removing the damaged part of the metatarsal head or phalanx base (19). This procedure alleviates pain and still allows for a range of motion; however, the amount of articulating surface remaining on the operated bony surface is reduced. Complications include

"floating hallux" and transfer metatarsalgia, or increased pressure/pain on the ball of the foot (19,32). Although this is a joint destructive procedure, enough of the bone remains to do a follow-up arthrodesis or implant arthroplasty at a later date, if needed (32).

FMTPJ Implant Designs

One of the first recorded attempts at FMTPJ implant arthroplasty was performed by Ender, who, in 1951, used an acrylic bone cement to re-create the base of a proximal phalanx (5). In 1952, Swanson fabricated a hemi-implant from metal to replace the head of the first metatarsal (5). In 1964, Seeburger introduced another hemi-implant, using Durallium® (a Ni-Co-Cr-Cu-Mg-Mn-Mo-Si alloy; www.lookchem.com) to create three different versions of the metatarsal head (5). Also, in 1964, Joplin used Vitallium (a Co-Cr-Mo alloy; www.lookchem.com) to create two different hemi-implant designs, one for the head of the metatarsal and the other for the base of the phalanx (5). In 1965, Swanson revised his original hemi-implant design by changing the material to silicone and, in 1967; he introduced a stemmed implant for the base of the phalanx, fabricating it from Silastic (5). A double-stemmed hinged implant, designed by Kampner, was introduced by a manufacturer, Cutter, in 1971 and, in 1974, another company, Dow Corning, introduced another of this type of implant; namely, the Swanson Flexible Hinge (5). The first multi-component implant, designed by Weil and Smith, was introduced in 1975 by Richards Manufacturing and comprised a stainless steel metatarsal component and an ultra-high molecular weight polyethylene (UHMWPE) phalanx component (5). The current generation of FMTPJ implants are, essentially, variants of these three types of designs; namely, hemi-, double-stemmed, and multi-component (Table 1).

Table 1. Some Features of a Sample of Current Generation FMTP Joint Implants

Manufacturer	Implant Name	Materials	Implant Type
Arthrosurface (Franklin, MA)	Hemi Cap	CoCr/Ti	Hemi-Phalanx
Ascension Ortho (Austin, TX)	Movement™ Great Toe System	CoCr/UHMWPE	Total
BioPro (Port Huron, MI)	Great Toe Hemi	CoCr	Hemi-Phalanx
Integra Life Sciences (Plainsboro, NJ)	K2 Hemi Toe Implant System	CoCr	Hemi-Phalanx
	KGTI Kinetic Great Toe Implant	CoCr/Ti/UHMWPE	Total
MetaSurge (Houston, TX)	Biomotion	Ti	Hemi-Phalanx
Moje Ceramic Implants (Petersberg, Germany)	Moje	Zirconium dioxide	Hemi-Metatarsal and Hemi-Phalanx
		Zirconium dioxide	Total
OrthoPro (Salt Lake City, UT)	Metal Hemi	CoCr/Ti Plasma	Hemi-Phalanx
Osteomed (Addison, TX)	Bioaction™ Great Toe Implant	CoCr/UHMWPE	Total
	Encompass™ Metatarsal Resurfacing Implant	CoCr/Ti Plasma/HA	Hemi-Metatarsal
	Hemi™ Great Toe Implant	CoCr	Hemi-Phalanx
	ReFlexion 1st MPJ Implant System	Ti/UHMWPE	Total
Sgarlato Medical (San Jose, CA)	GAIT GTI	Silicone	Hinged
Smith & Nephew (Baar, Switzerland)	Toefit Plus™	Ti/UHMWPE	Total
Tornier (Edina, MN)	Futura™ Primus	Silicone/Ti Grommets	Hinged
	Futura™ Classic	Silicone	Hinged
	Futura™ Metal Hemi	CoCr	Hemi-Phalanx
Trilliant (Houston TX)	3S Hemi Implant	CoCr	Hemi-Phalanx
Wright Medical (Arlington, TN)	LPT Great Toe Implant	Ti	Hemi-Phalanx
	Swanson Flexible Hinge Toe	Silicone/Ti Grommets	Hinged
Vilex (McMinnville, TN)	CHI™	CoCr or Ti	Hemi-Metatarsal and Hemi-Phalanx

Design, Operation, and Stress Analysis

Design Requirements for the Wear Tester

ISO 14242 (3) and ISO 14243 (4) are international standards for wear testing hip and knee implants. Using these standards as guides and results given in literature reports regarding the range of motion and forces experienced by the FMTPJ during the normal gait cycle, the following were identified as the design requirements for the wear tester:

1. Implant to be immersed in bovine solution, at 37 ^{o}C.(3,4)
2. Implant to be subjected to a loading cycle at a frequency of 1 Hz.(3,4)
3. Range of motion to be no less than 40^{o}.(18,21,22)
4. Capable of applying force of at least 600 N during articulation.(1,15)
5. Mounting for implant must be adaptable to accommodate any type of implant (Table 1)

Details of the Designed Wear Tester

Solid models of the various components of the wear tester were created using a commercially-available software package (Pro-E Wildfire 3.0; PTC, Needham, MA) and are presented in Figures 6-9. The list of materials for the machine components is given in Table 2 and a 2D schematic drawing is shown in figure 5. Minus any engineering and programming fees, the tester should cost around $15,000 to build.

The wear tester will contain four stations; one station provides the static load for the control implant while the other three provide load plus articulation for the implant under test. By placing the articulating arms overhead and mounting the specimen on a dropped mount, 40^{o} of articulation will be possible. A motor attached to a 90^{o} gear box and mounted to one of the articulating stations will provide the motion. The hydraulic

piston, located at the base of each station, will be attached to a load cell that will provide feedback to the pump. This will provide the requisite load of 600 N.

Table 2. List of basic components of the wear tester.

Component	Material	Qty
Machine Base	6061-T6 Al alloy	1
Machine Side	6061-T6 Al alloy	2
Articulating Arm	6061-T6 Al alloy	8
Articulating Cross-member	6061-T6 Al alloy	4
Drop Mount	6061-T6 Al alloy	4
Mounting Base	6061-T6 Al alloy	4
Metatarsal Implant Mount	ABS-Like SLA	4
Phalangeal Implant Mount	ABS-Like SLA	4
Serum Cup	UHMWPE/Polycarbonate	4
Load Cell	Various	4
Load Cell Mount	6061-T6 Al alloy	4
Hydraulic/pneumatic Piston	Various	4
Articulating Lever	6061-T6 Al alloy	3
Lever Actuator	6061-T6 Al alloy	1
1kw Motor	Various	1
90^{o} Gearbox	Various	1
Controller		2
Software		
Pump w/heated bath		1

ABS: acryl obutyl styrene; SLA: stereolithography

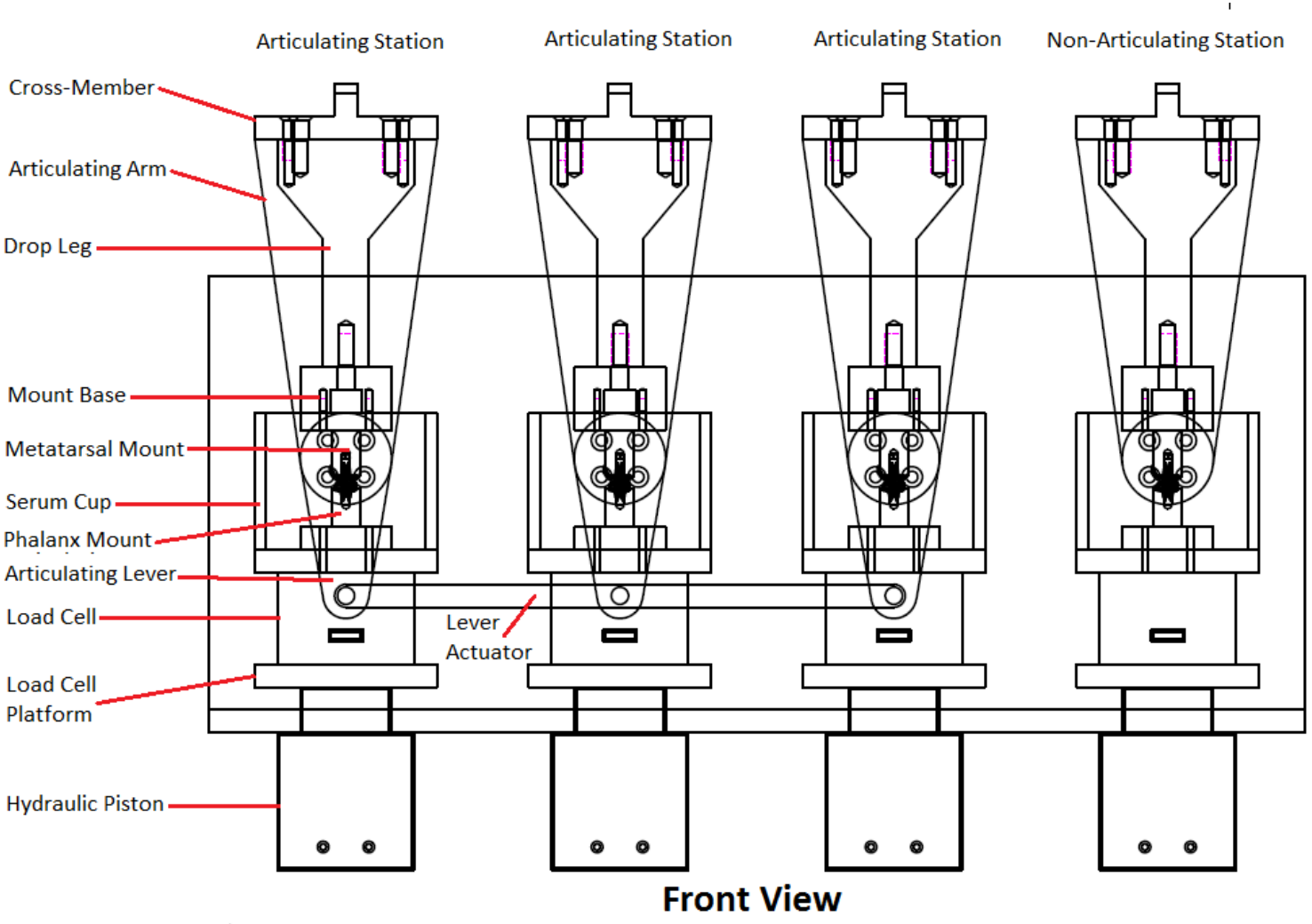

Figure 5. 2D Schematic Drawing of Wear Tester

A solid model of the assembled designed wear tester is presented in Figure 6. Outside overall dimensions are approximately 24” wide, 9” deep and 17 ¼” tall, not including the motor/gearbox or cabinet. Articulation occurs in the dorsiflexion range to 40^{o}, away from the static load station to allow for clearance. The motor/gear box assembly will mount to the rotational axis of the center articulating station, which will then drive the remaining articulating stations.

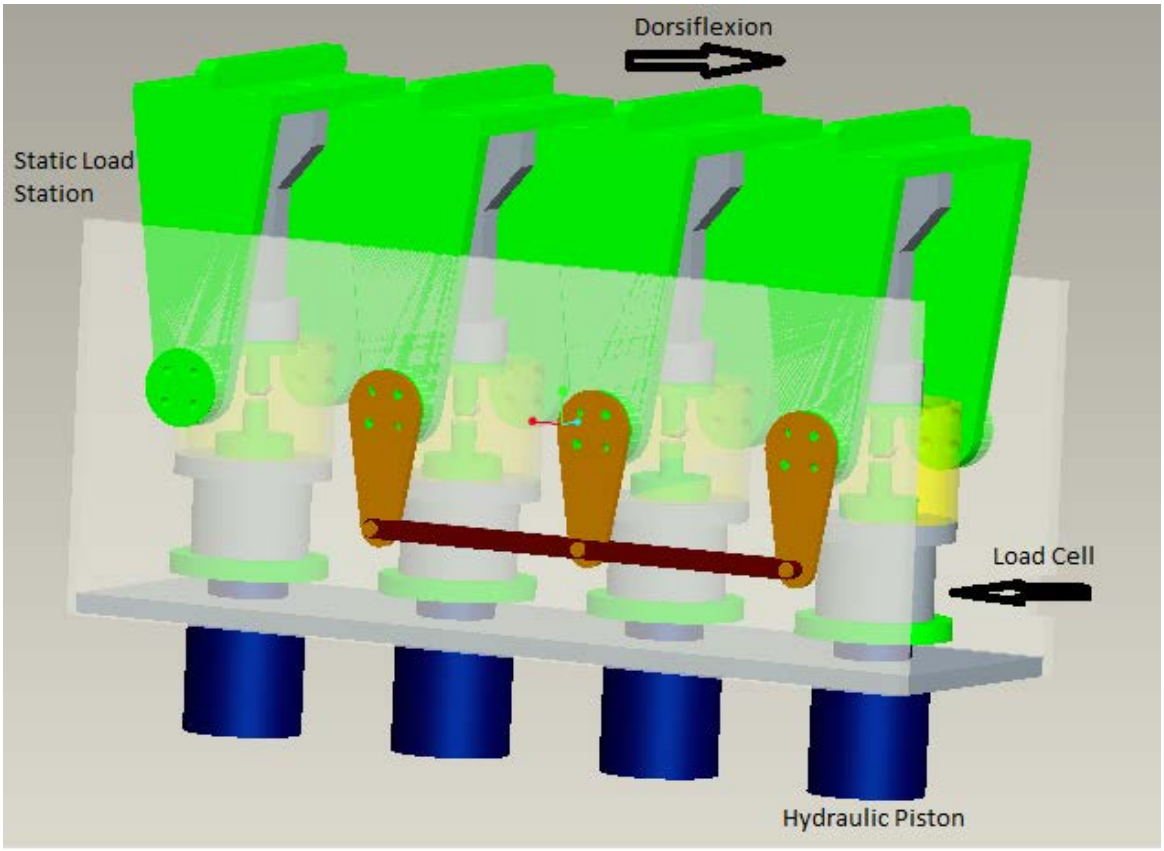

Figure 6. Solid Model of the Assembled Wear Tester

A cut-away model showing the implant, located in the first of the articulating stations, is presented in Figure 7. The overhead mount allows for complete immersion of the implant in the bovine serum, which can be pumped in from the open top to maintain the required 37^{o} C. The center of rotation of the metatarsal component is lined up with the center of rotation of the articulating arm.

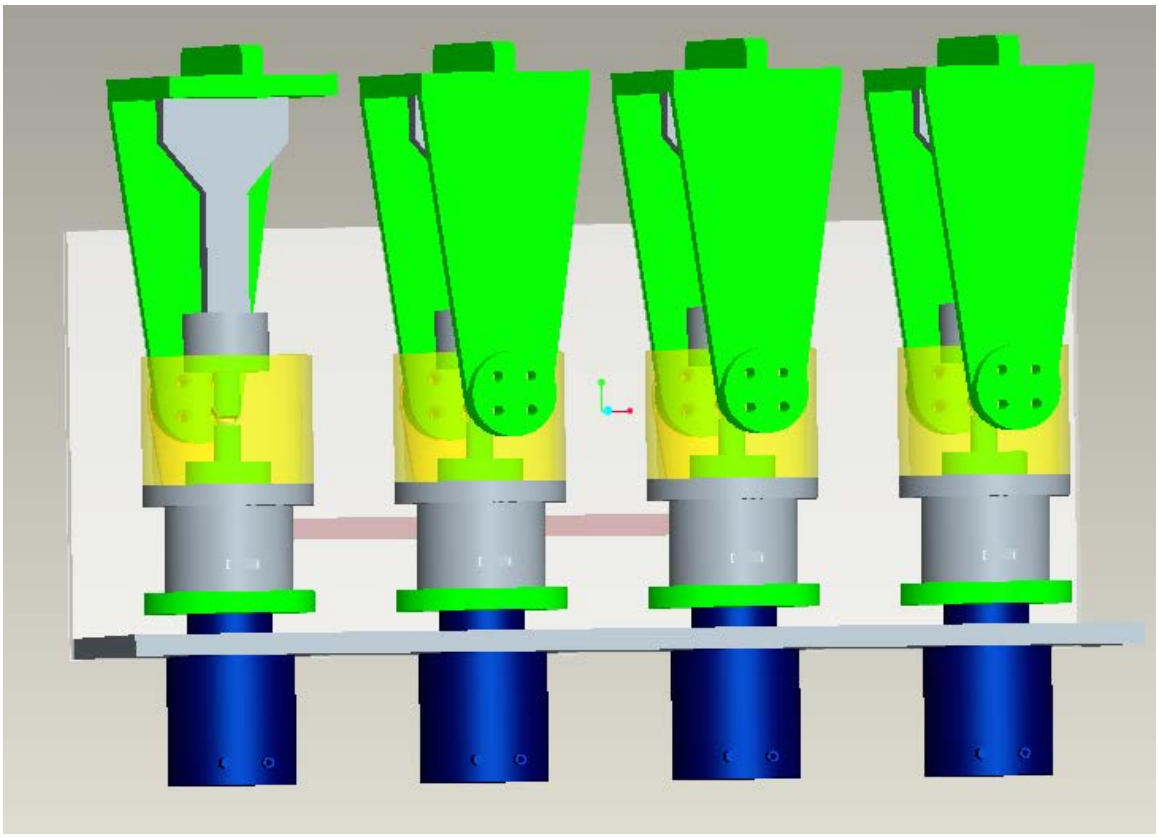

Figure 7. Solid Model of Cut-Away View of One of the Articulating Stations

A close-up of the metatarsal component resting on the surface of the UHMWPE insert to the phalanx component is given in Figure 8. The metatarsal component mount can be shimmed or shaved to insure proper alignment to the center of rotation. The hydraulic piston provides the lift to bring the phalanx component into contact with the metatarsal component.

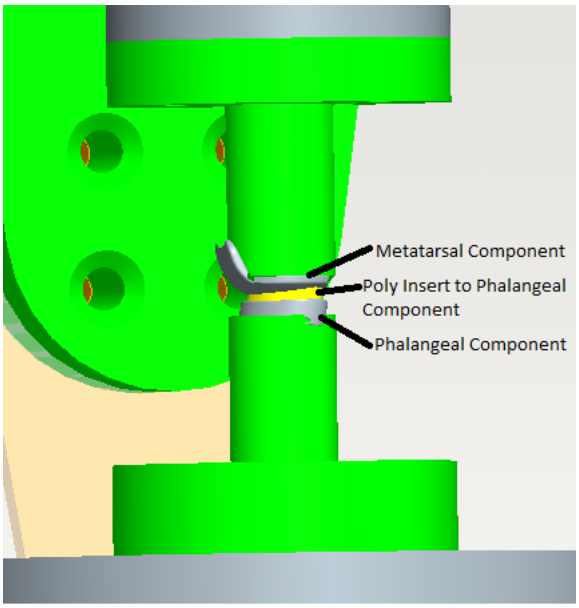

Figure 8. Solid Model: Close-Up View of Implant Mounted in the Wear Tester

Solid models of the key components that allow the wear tester to be adaptable to different types of implants (Table 1) are given in Figure 9. The dynamic components of the machine were designed to mimic the biomechanics of the FMTPJ. The component mounts are disposable pieces created using a rapid prototyping method, such as stereolithography. For each implant to be tested, a solid model will be created using a commercially-available software package or acquired from the manufacturer. The model will then be used to create the cavity in the mount and then the length of the mount will

be adjusted to line up the center of rotation of the implant to that of the tester. The implant will be mounted in the wear tester fixtures in the same way as is done during an implantation procedure; that is, cemented in a bed of acrylic bone cement or press fitted.

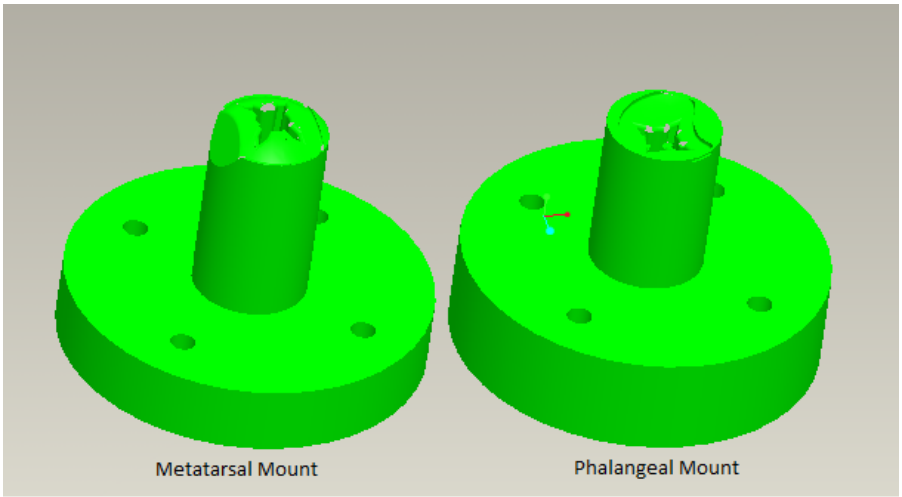

Figure 9. Solid Models of the Component Mounts

Operation of the Designed Wear Tester

The dynamic components of the wear tester will be controlled with motors, encoders, controllers, and software. An electric motor rating: 1kW, mounted to a 90^{o} speed reduction gearbox, will provide enough torque to articulate the overhead arms. This assembly will attach to one of the articulating stations, which will then drive a lever to articulate the other two articulating stations. Commercially-available software package such as FlexTest® (MTS; Eden Prairie, MN), Pro-Motion® (PMD; Boxborough, MA), or Visual Basic® (Microsoft; Redmond WA), will be used to program the controllers. This software will read the information from the encoder to set amount of desired articulation, the frequency of that articulation, as well as keeping up with the cycle count. At the same time, the software will be tasked to control the pressure on the hydraulic pistons during

key angles of articulation, by reading the feedback from the load cells and controlling the pressure created by the hydraulic pump. This will cycle from almost no pressure at 0^o articulation and increase to the desired load as peak articulation is reached.

Stress Analysis of an Articulating Test Station

A commercially-available finite element analysis (FEA) package (ANSYS 11.0; ANSYS Inc., Canonsburg, PA) was used to perform the stress analysis of an articulating test station, at 0^o articulation as well as at 40^o articulation, to represent the full range of motion that would be experienced by an implant during a wear test. The finite element meshes of the station, at each of these articulations, obtained using tetrahedral elements (17,711 Elements, 35,891 Nodes), are shown in Figures 10 and 11, respectively. Note the high mesh density of the ABS-Like SLA fixture in recognition of the fact that the fixture is expected to be the weakest component in the tester. Subsequent analyses were run using more refined mesh sizes and a higher stressed element, located in the transition between the shaft and taper on the drop leg, was followed to test for convergence. Table 3 lists the mesh details and the equivalent stress at the observed element. Little difference was seen in the results so the original mesh was sufficient to produce accurate results.

Table 3. Results from Convergence Test

Mesh Details	# of Elements # of Nodes	von-Mises stress at transition point of drop leg [MPa]
Course	17,711 35,891	42.855
Medium	24,743 59,262	48.373
Fine	32,727 93,451	46.909

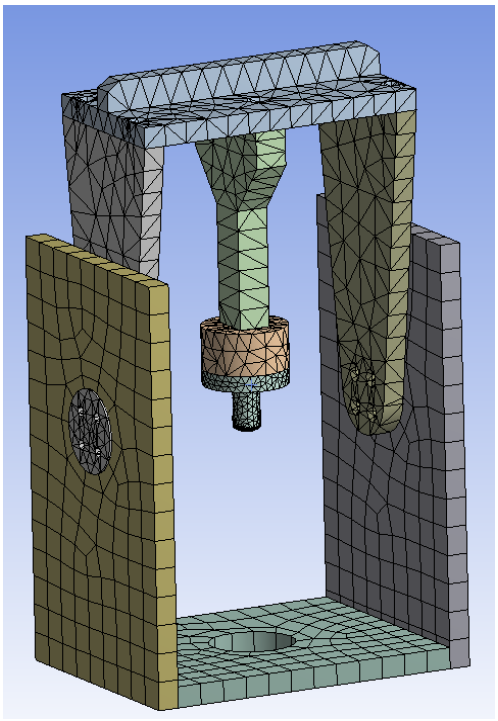

Figure 10. 0^{o} Meshed Structure

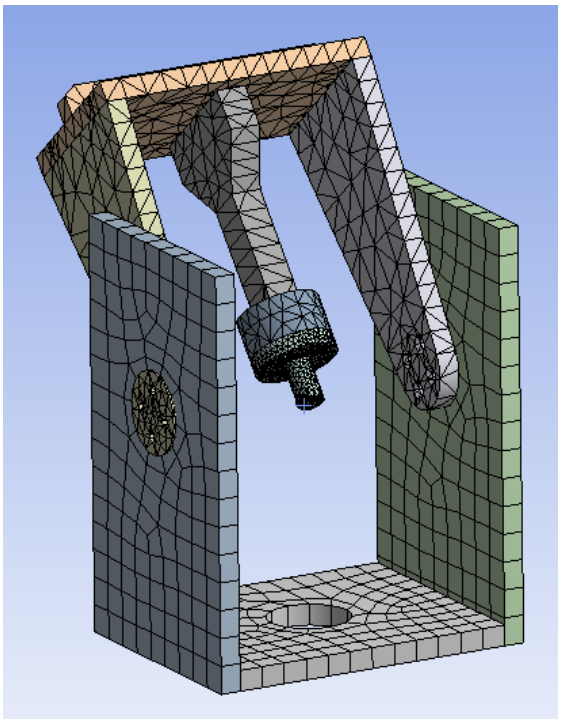

Figure 11. 40^{o} Meshed Structure

For the analysis, a force of 1200 N was applied to the surface of the implant (Figures 12 and 13). This force magnitude is twice what would be used during a test. There are two reasons for this approach. First, it would allow investigation of the load capacity of the wear tester. Second, it will allow evaluation of FMTPJ implants under load conditions the joint experiences in activities other than normal gait. Note the mesh display was turned off to highlight the direction of the applied load.

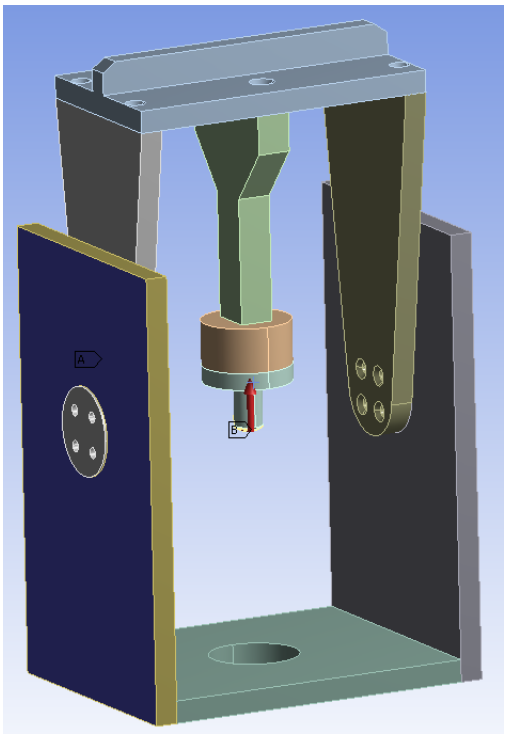

Figure 12. 0^{o} 1200 N Load

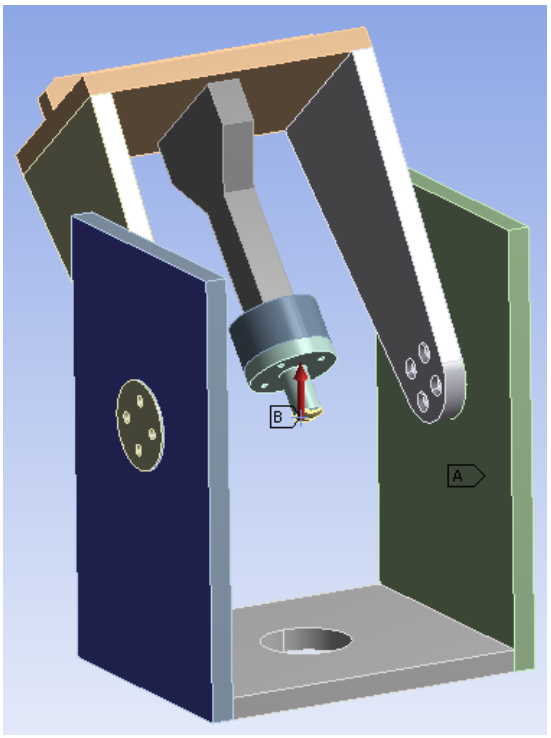

Figure 13. 40^{o} 1200 N Load

Two key features of the von Mises stress contours for all the components in the articulating test station, at 0^{o} and 40^{o} articulations (Figures 14 and 15) are noted. First, the highest stress is at the implant-fixture interface, a finding that might help explain why implant loosening is such a prevalent failure mode for the FMTPJ implants (10,28). Second, the highest stress experienced in each of the other parts of the station is much lower than the yield strength of 6061-T6 Al alloy (276 MPa; E=69GPa; υ=0.3) (39), which indicates the high factor of safety of the station against elastic failure, when subjected to a quasi-static load.

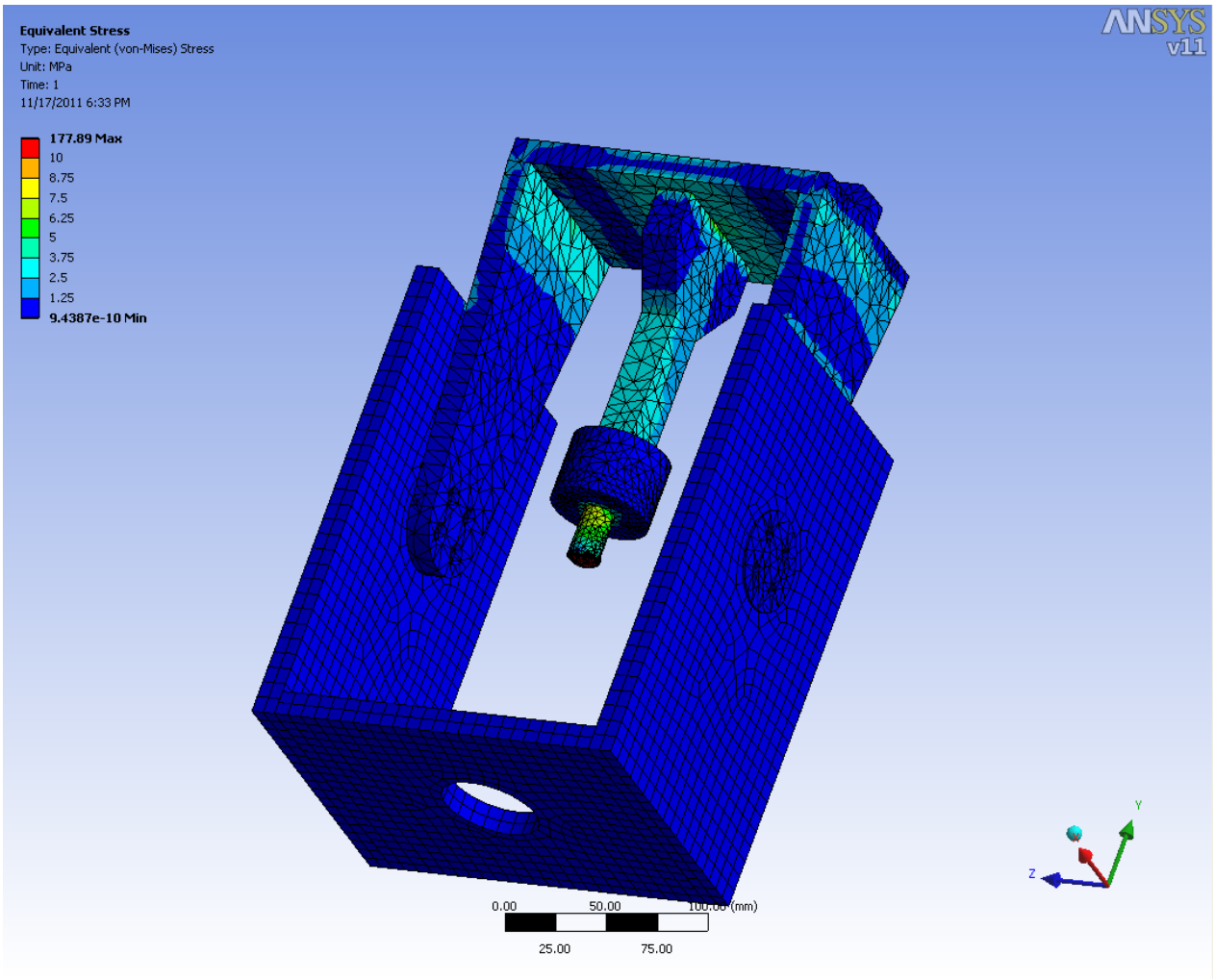

Figure 14. von Mises Stress Contour for a Test Station, at 0^{o} Articulation.

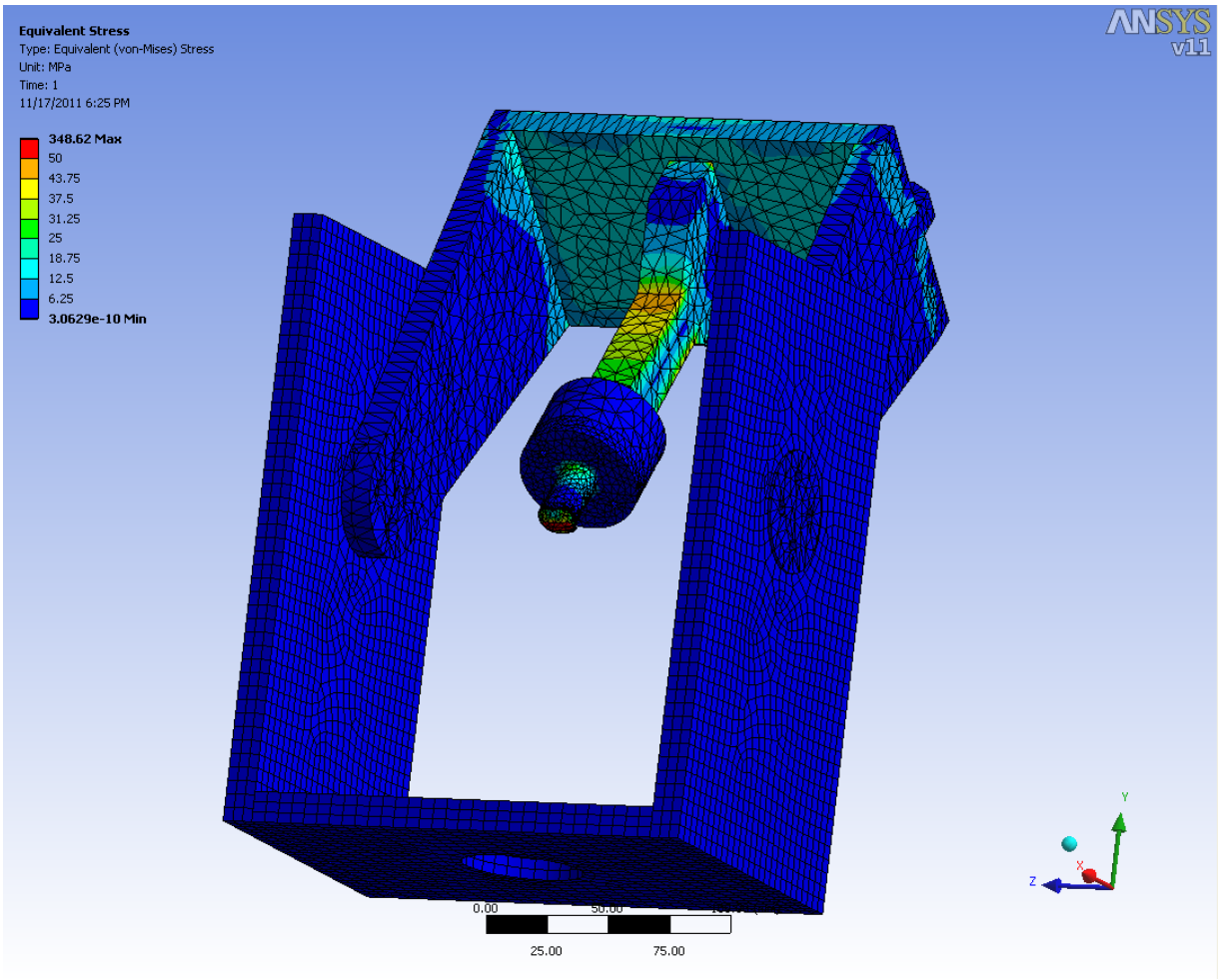

Figure 15. von Mises Stress Contour for a Test Station at 40^{o} Articulation.

Proposed Wear Test Protocol

For a given implant, one control specimen and three test specimens should be used. All specimens should be cleaned and weighed in a way that is similar to what is specified in ISO 14243-2 (4). The control specimen will be placed under the same load and in the same environment as the test specimens but not articulated during the test. Thus, the control specimen will be used as a reference to determine weight gained while being immersed in the bovine serum over the period of the test. The test specimens will be placed under a 600 N load and articulated through 40^{o} of dorsiflexion at a frequency of

1 Hz. Test specimens should be removed, cleaned, and weighed and the bovine serum replaced every 500,000 to 1,000,000 cycles, until test is complete. Test will be complete upon implant failure or after 5,000,000 cycles, whichever comes first.

At the end of the test, the test specimen should be carefully cleaned, dried in a vacuum oven, and weighed. Its loss of mass will then be corrected using the mass gain/loss of the control specimen. The wear rate of the test specimen could then be expressed in, for example, corrected loss of mass of implant (in mg) per 1 million loading cycles.

As far as acceptance criteria are concerned, these should be developed by studying clinical results and analyses of explanted prostheses (6). This type of development is not uncommon when developing a new tester and evaluating the wear test results. Bell and Fisher developed a new wear tester for an ankle joint prosthesis, but had no existing data with which to compare their results (33). They tested an ankle implant with a good clinical history to establish a baseline for a new design (33). Ellison et al developed an *in vitro* wear tester for patellofemoral implants and tested designs currently in clinical use (34). They then compared their results against explanted specimens to determine the validity of their tester (34).

Caution should be exercised when developing acceptance criteria as it is known that *in vitro* wear test results from THJRs and TKJRs do not always reflect clinical results. Potentially, *in vitro* testing could lead to improved outcomes because it is carried out in a controlled environment with repeatable fixturing, movements and forces. Whereas it is easy to pinpoint excessive deformation or fracture of an implant, how much mass loss the implant can experience and still function properly is somewhat subjective.

Some observed wear rates of UHMWPE tibia inserts in TKJRs have been measured in the range of 3.9 mm^3 per million to 41.0 mm^3per million cycles, with no mention of prediction of lifespan (35). The wear rate for these implants is expected to be higher than what would be observed in FMTPJ implants due to the large size of the femoral components and the high amount of surface area contact in the knee.

An alternative to studying explants is radiographic evaluation of the implant *in vivo*. Kendrick et al. performed an *in vivo* wear test study on unicompartmental KJRs using patient radiographs to measure the linear penetration of the UHMWPE tibia insert after an average of 20.9 years post implantation (36). They determined that the average linear penetration of the insert was 1.04 mm, or 0.045mm/year (36).[35] A similar type of measurement method could be applied to analyzing results of *in vitro* wear tests on a FMTPJ implant to see if the results obtained are similar to those observed clinically.

Conclusions and Recommendations for Future Study

The first metatarsophalangeal joint (FMTPJ) is prone to many types of disorders/diseases, notably, osteoarthritis and rheumatoid arthritis. In cases where the pain due to a disease has not been relieved through the use of a conservative measure, such as ingestion of an analgesic, or the disease is at an advanced stage, the usual treatment option is arthrodesis. This option does, however, have a major limitation in that it results in complete loss of motion at the joint. An alternative surgical method involves insertion of an implant at the joint. Although there are many designs of FMTPJ implants in clinical use, there are no literature reports on the design of FMTP implant wear testers. In the present work, we designed such a tester, in which the implant under test will be 1) housed in a chamber that contains bovine serum, at 37 ^{o}C, and 2) articulated at no less than 40^{o} dorsiflexion under a cyclic 600 N loading, at a frequency of 1 Hz. Furthermore, the designed tester will be capable of testing any type of FMTPJ implant. Stress analysis revealed that the highest stress occurs at the implant/fixture interface. Dividing the material yield strength of 276MPa by the lowest and highest calculated equivalent stresses on the remaining components, resulted in a factor of safety range of 5 to 126. Various aspects of a wear test protocol, using the designed tester, as well as acceptance criteria, based on clinical results, are presented.

Future work should be directed to validating results obtained using the designed wear tester, for a wide collection of current-generation FMTPJ implants. Additional FEA work should include analysis based on a dynamically applied load, as we only covered static loading. Results are likely to change depending on the implant type and material being tested. Validation of the software generated FEA results for deflection should be

performed once the tester is built. Finished components can be measured for actual deflection using resistance strain gages and the measured results can be compared with the calculated results.

References

1. Jacob HAC. Forces acting in the forefoot during normal gait – an estimate. Clin Biomech 16:783-792, 2001.

2. Gomez PF, Morcuende JA. Early Attampts at Hip Arthroploasty-1700s to 1950s. Iowa Orthop J 25:25-29, 2005.

3. ISO 14242. Implants for Surgery-wear of total hip joint prostheses, parts 1 & 2. ISO, Geneva, 2002.

4. ISO 14243. Implants for Surgery-wear of total knee-joint prostheses-part 2: methods of measurement. ISO. Geneva, 2009.

5. Hetherington VJ, Cwikla PS, Malone M. Review of first metatarsophalangeal joint implants. Hallux Valgus & Forefoot Surgery. Churchill Livingstone Ch 25:347-358, 1994.

6. Joyce TJ. Implants for the first metatarsophalangeal joint and prospective considerations. Ex Rev Med Devices 2(4):453-464, 2005.

7. Sung W, Weil L Jr., Weil LS Sr., Stark T. Total first metatarsophalangeal joint implant arthroplasty: A 30-year retrospective. Clin Pod Med Surg 28:755-761, 2011.

8. Joyce TJ. Examination of failed ex vivo metal-on-metal metatarsophalangeal prosthesis and comparison with theoretically determined lubrication regimes. Wear 263:1050-1054, 2007.

9. Ghalambor N, Cho DR, Goldring SR, Nihal A, Trepman E. Microscopic metallic wear and tissue response in failed titanium hallux metatarsophalangeal implants: two cases. Foot Ankle Int 23(2):158-162, 2002.

10. Nixon MF, Taylor GJS. Early failure of the Moje implant when used to treat hallux rigidus: The need for regular surveillance. Int J Clin Foot Science 18(1):1-6, 2008.

11. Nordin M, Frankel VH. Basic biomechanics of the musculoskeletal system. 3rd Ed. Lippincott Williams & Wilkins, 2001.

12. Logan BM, Singh D, Hutchings RT. McMinn's color atlas of foot & ankle anatomy. 3rd Ed. Mosby. 2004

13. Flavin R, Halpin T, O'Sullivan R, FitzPatrick D, Ivankovic A, Stephens M M. A finite-element analysis study of the metatarsophalangeal joint of the hallux rigidus. J Bone Joint Surg Br 90-B:1334-1340, 2008.

14. http://academic.kellogg.edu/herbrandsonc/bio201_mckinley/f8-15a_right_foot_media_c.jpg, 2011.

15. Stokes IAF, Hutton W, Stott JRR. Forces acting on the metatarsals during normal walking. J Anat 129(3):579-590, 1979.

16. Oloff LM, Feist MA. First metatarsophalangeal implants. Hallux Valgus & Forefoot Surgery. Churchill Livingstone Ch. 24:327-346, 1994.

17. Carson MC, Harrington ME, Thompson N, O'Connor JJ, Theologis TN. Kinematic analysis of a multi-segment foot model for research and clinical applications: a repeatability analysis. J Biomech 34:1299-1307, 2001.

18. Nawoczenski DA, Baumhauer JF, Umberger BR. Relationship between clinical measurements and motion of the first metatarsophalangeal joint during gait. J Bone Joint Surg 81-A(3):370-376, 1999.

19. Kim PJ, Hatch D, DiDomenico LA, Lee MS, Kaczander B, Count G, Kravette M. A multicenter review of outcomes for arthrodesis, hemi-metallic joint implant, and resectional arthroplasty in the surgical treatment of end-stage hallux rigidus. J Foot Ankle Surg In Press:1-7, Submitted 2011.

20. Waizy H, Czardybon MA, Stukenborg-Colsman C, Wingenfeld C, Wellmann M, Windhagen H, Frank D. Mid- and long-term results of the joint preserving therapy of hallux rigidus. Arch Orthop Trauma Surg 130:165-170, 2010.

21. Halstead J, Turner DE, Redmond AC. The relationship between hallux dorsiflexion and ankle joint complex frontal plane kinematics: A preliminary study. Clin Biomech 20:526-531, 2005.

22. Hetherington VJ, Chessman GW, Steuben C. Forces on the first metatarsophalangeal joint: a pilot study. J Foot Surg 31(5):450-453, 1992.

23. Brewster M. Does total joint replacement or arthrodesis of the first metatarsophalangeal joint yield better functional results? A systematic review of the literature. J Foot Ankle Surg 49:546-552, 2010.

24. Cusumano T, DPM. How to treat osteoarthritis of the first MTPJ. Pod Today 17(3):28-32, 2004.

25. Zang K, Askari S, Fuller A, Seuferling C. First metatarsal pathology: Can an implant provide a long-term solution?. Pod Today 19(3):35-43, 2006.

26. Vanore JV, Christensen JC, Kravitz SR, Schuberth JM, Thomas JL, Weil LS, Zlotoff HJ, Couture SD. Diagnosis and treatment of first metatarsophalangeal joint disorders. Sections 1-6. J Foot Ankle Surg 42(3):112-154, 2003.

27. Torkki M, Malmivaara A, Seitsalo S, Hoikka V, Laippala P, Paavolainen P. Surgery vs orthosis vs watchful waiting for hallux valgus. J Am Med Assoc 285(19):2474-2480, 2001.

28. Gibson JN, Thomson CE. Arthrodesis or total replacement arthroplasty for hallux rigidus: a randomized controlled trial. Foot Ankle Int 26(9):680-690, 2005.

29. Cook E, Cook J, Rosenblum B, Landsman A, Giurini J, Basile P. Meta-analysis of first metatarsophalangeal joint implant arthroplasty. J Foot Ankle Surg 48(2):180-190, 2009.

30. Harvard Pilgrim Health Care. Medical Policy Partial for Total Replacement of First Metatarsophalangeal Joint. Boston, MA. Nov 2009.

31. CIGNA Medical Coverage Policy #0446. Metatarsophalangeal Joint Replacement. Bloomfield, CT. March 2011.

32. Simpson-White RW, Joseph G, Khan MZGM. Prosthetic replacement arthroplasty as a salvage operation for failed procedures of the first metatarsophalangeal joint: A small series and literature review. The Foot 17:174-177, 2007.

33. Bell CJ, Fisher J. Simulation of polyethylene wear in ankle joint prostheses. J Biomedical Mat Res Part B: App Biomater 81(1):162-167, 2007.

34. Ellison P, Barton DC, Esler C, Shaw DL, Stone MH, Fisher J. In vitro simulation and quantification of wear within the patellofemoral joint replacement. J Biomech 41:1407-1416, 2008.

35. McEwen HMJ, Barnett PI, Bell CJ, Farrar R, Auger DD, Stone MH, Ficher J. The influence of design, materials and kinematics on the in vitro wear of total knee replacements. J Biomech 38:357-365, 2005.

36. Kendrick BJL, Simpson DJ, Kaptein BL, Valstar ER, Gill HS, Murray DW, Price AJ. Polyethylene wear of mobile-bearing unicompartmental knee replacement at 20 years. J Bone Joint Surg Br 93-B(4):470-475, 2011.

37. Ess P, Hamalainen M, Leppilahti J. Non-constrained titanium-polyethylene total endoprosthesis in the treatment of hallux rigidus: A prospective clinical 2-year follow-up study. Scand J Surg 91:202-207, 2002.

38. http://www.clinicalgaitanalysis.com, 2011.

39. Budinski KG, Budinski MK. Engineering Materials: Properties and Selection. 9th Ed. Prentice Hall, 2010.